Supplementary Information (SI) for Sensors & Diagnostics.
This journal is © The Royal Society of Chemistry 2025

# Bimodal Sensor Employing a Novel Approach for Simultaneous Selective Detection of $Ni^{2+}$ and Biomolecules via Turn-On Fluorescence Supported by DFT and Molecular Docking

*Hazeena Shinziya[a], Avijit Kumar Das[a]*, Malavika S Kumar[a], Anish Nag[b], Malay Dolai[c]*

[a]Department of Chemistry, Christ University, Hosur Road, Bangalore, Karnataka, 560029 India, *Email: avijitkumar.das@christuniversity.in

[b]Department of Life Science, Christ University, Hosur Road, Bangalore, Karnataka, India, 560029

[c]Department of Chemistry, Prabhat Kumar College, Contai, Purba Medinipur 721404, W.B., India.

## CONTENTS

# 1. Experimental

## 1.1. General:

Unless otherwise mentioned, chemicals and solvents were purchased from Sigma-Aldrich chemicals Private Limited and were used without further purification. $^{1}$H-NMR spectra were recorded on Brucker 400 MHz instrument. For NMR spectra, DMSO was used as solvent using TMS as an internal standard. Chemical shifts are expressed in $\delta$- units and $^{1}$H–$^{1}$H and $^{1}$H–C coupling constants in Hz. UV-vis titration experiments were performed on a UV-Spectrophotometer: PerkinElmer, Lambda 30 and fluorescence experiment was done using Shimadzu RF-6000 Fluorescence spectrofluorometer using a fluorescence cell of 10 mm path.

## 1.2. General method of UV-vis and fluorescence titration:

**By UV-vis method:**

For UV-vis titrations, stock solution of the sensor was prepared ($c$ = 2 x $10^{-5}$ M) in $CH_3CN$-HEPES buffer (7/3, v/v, 25°C) at pH 7.4. The solution of the guest interfering analytes like $Cu^{2+}$, $Mn^{2+}$, $Pb^{2+}$, $Cd^{2+}$, $Fe^{2+}$, $Cu^{2+}$, $Fe^{3+}$, $Zn^{2+}$, $Co^{2+}$, $Al^{3+}$, $Cr^{3+}$, $Ni^{2+}$ as their chloride salts were also prepared in the order of $c$ = 2×$10^{-4}$M. Solutions of various concentrations containing sensor and increasing concentrations of cations were prepared separately. The spectra of these solutions were recorded by means of UV-vis methods.

For UV-*vis* titrations of **DSM** with ct-DNA, BSA and ovalbumin, the stock solution of the sensor ($c$ = 2× $10^{-5}$ M) was prepared in DMSO- Tris-HCl buffer (40 µL in 2 ml Tris-HCl buffer) at pH 7.2. And tris-HCl buffer was used to prepare the solution of ct-DNA ($c$ = 2 mM in base pairs), BSA ($c$ = 7.4 µM) and ovalbumin ($c$ = 4.24 µM). The spectra of these solutions were recorded by means of UV-vis methods.

**General procedure for drawing Job plot by UV–vis method:**

Stock solution of same concentration of **DSM** and $Ni^{2+}$ were prepared in the order of ≈ 2.0 x $10^{-5}$ M in $CH_3CN$-HEPES buffer (7:3, v/v, pH = 7.4). The absorbance in each case with different *host–guest* ratio but equal in volume was recorded. Job plots were drawn by plotting $\Delta I.X_{host}$ *vs* $X_{host}$ ($\Delta I$ = change of intensity of the absorbance spectrum during titration and $X_{host}$ is the mole fraction of the host in each case, respectively).

**By fluorescence method:**

For fluorescence titrations, stock solution of the sensor ($c$ = 2 x $10^{-5}$ M) was prepared for the titration of cations in $CH_3CN$-HEPES buffer [7:3, v/v, pH = 7.4]. The solution of the guest

cations using their chloride salts in the order of 200 μM were also prepared. Solutions of various concentrations containing sensor and increasing concentrations of cations were prepared separately. The spectra of these solutions were recorded by means of fluorescence methods.

For UV-*vis* titrations of **DSM** with ct-DNA, BSA and ovalbumin, the stock solution of the sensor ($c = 2\times 10^{-5}$ M) was prepared in DMSO- Tris-HCl buffer (40 μL in 2 ml Tris-HCl buffer) at pH 7.2. And tris-HCl buffer was used to prepare the solution of ct-DNA ($c$ = 2 mM in base pairs), BSA ($c$ = 7.4 μM) and ovalbumin ($c$ = 4.24 μM). The spectra of these solutions were recorded by means of UV-vis methods.

## 2.Viscosity Studies:

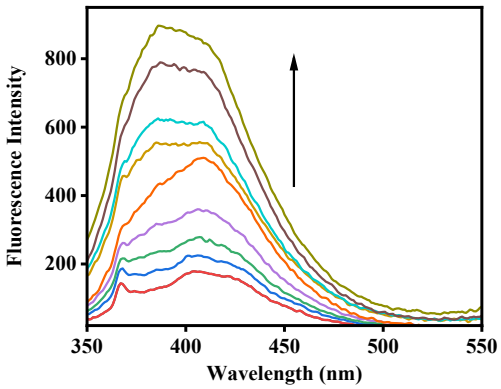


**Figure S1.** (a) Fluorescence spectra of **DSM** ($c = 2.0 \times 10^{-5}$ M) in methanol-glycerol solution with different viscosity with various glycerol percentage.

## 3. Binding constant determination:

The binding constant value of cation $Ni^{2+}$ with the sensor has been determined from the emission intensity data following the modified Benesi–Hildebrand equation, $1/\Delta I = 1/\Delta I$ max + (1/K[C])(1/ΔI max). Here ΔI = I-Imin and ΔI max = Imax-Imin, where Imin, I, and Imax are the emission intensities of sensor considered in the absence of guest, at an intermediate concentration and at a concentration of complete saturation of guest where K is the binding constant and [C] is the guest concentration respectively. From the plot of (Imax-Imin)/(I-Imin) against $[C]^{-1}$ for sensor, the value of K has been determined from the slope. The binding constant ($K_a$) as determined by fluorescence titration method for sensor with $Ni^{2+}$ is found to be $1.2 \times 10^6$ $M^{-1}$ (error < 10%).

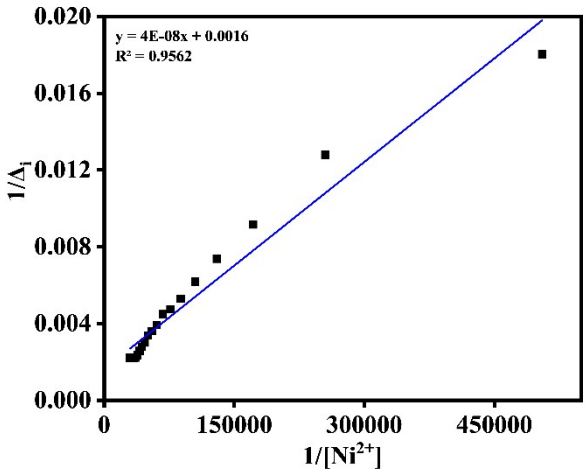


**Figure S2.** Benesi–Hildebrand plot from fluorescence titration data of receptor (20μM) with $Ni^{2+}$ [G].

The binding constants of **DSM** with ct DNA, BSA and ovalbumin were determined from the fluorometric titration spectra by fitting of the experimental data to the theoretical model in the following equation:[1]

$$\frac{I}{I_0} = 1 + \frac{Q-1}{2}\left(A + xn + 1 - \sqrt{(Q + xn + 1)^2 - 4xn}\right) \quad \text{(Equation 1)}$$

where $Q = I/I_0$ is the minimal emission intensity in the presence of excess ligand; $n$ is the number of independent binding sites per DNA or proteins;

9. $= 1/ (K_b \times C_{DSM})$;

$x = C_{DNA\ or\ protein}/C_{DSM}$ is the titration variable

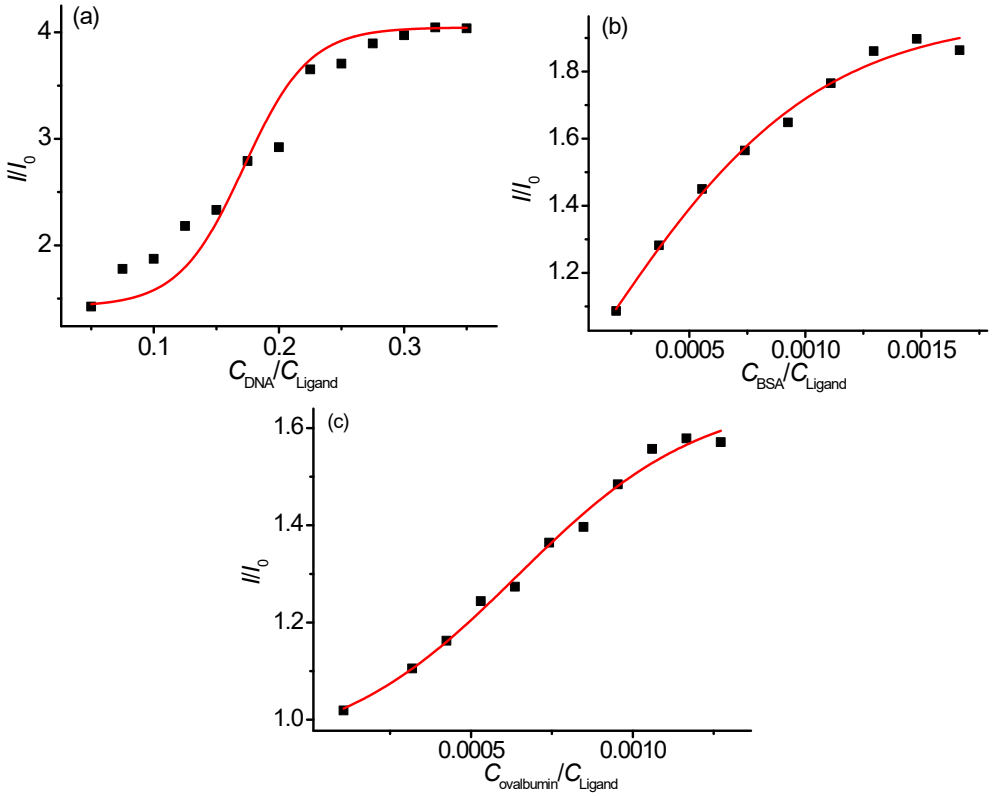


**Figure S3.** Non-linear fitting curves of binding isotherms from spectrofluorometric titrations of **DSM** with (a) ct-DNA (b) BSA and (c) ovalbumin. Red lines represent the best fits to the theoretical model.

## 4. Determination of fluorescence quantum yield:

Here, the quantum yield φ was measured by using the following equation,

$\varphi_x = \varphi_s (Fx / F_s) (As / A_x) (n_x^2 / n_s^2)$

Where,

X & S indicate the unknown and standard solution respectively, φ = quantum yield,

F = area under the emission curve, A = absorbance at the excitation wave length,

n = index of refraction of the solvent. Here φ measurements were performed using anthracene in ethanol as standard [φ = 0.27] (error ~ 10%).

## 5. Calculation of the detection limit (DL):

The detection limit DL of **DSM** for $Ni^{2+}$ was determined from the following equation:

DL = K* Sb1/S

Where K = 2 or 3 (we take 3 in this case); Sb1 is the standard deviation of the blank solution; S is the slope of the calibration curve.

From the graph Fig.S4, we get slope = 14.35, and Sb1 value is 7.26

Thus, using the formula we get the Detection Limit for $Ni^{2+}$ = 1.53 μM

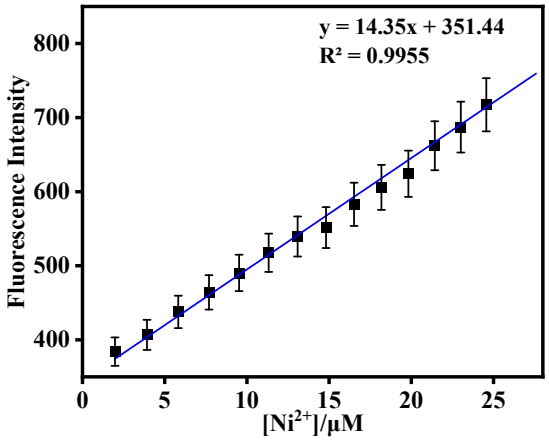


**Figure S4.** Changes of Fluorescence Intensity of **DSM** as a function of [$Ni^{2+}$] at 380 nm.

The detection limits (DL) of **DSM** with DNA, BSA and ovalbumin were determined from the following equation:

DL = K* Sb1/S

Where K = 2 or 3 (we take 3 in this case); Sb1 is the standard deviation of the blank solution; S is the slope of the calibration curve.

From UV-*vis* (a) and fluorescence titration (b) of **DSM** with ct-DNA (Fig.S5), slope values are -10732, 109.21 and Sb1 values as 0.001, 37.06 respectively.

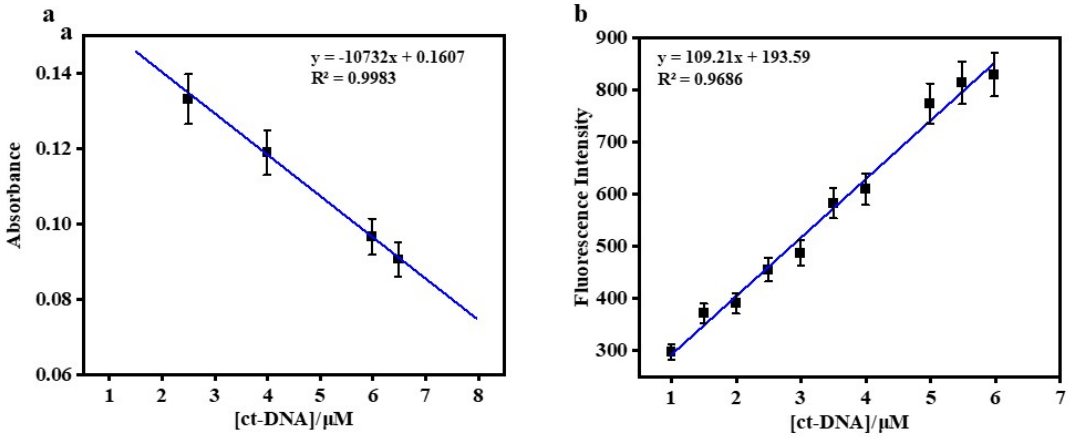


**Figure S5.** Changes of absorbance (a) and emission (b) of **DSM** ($c$ = 2.0 × $10^{-5}$ M) upon addition of ct DNA ($c$ = 2mM in base pairs).

From UV-*vis* (a) and fluorescence titration (b) of **DSM** with BSA (Fig.S6), slope values are -3.534, 12989 and Sb1 values are 0.009, 7.333 respectively.

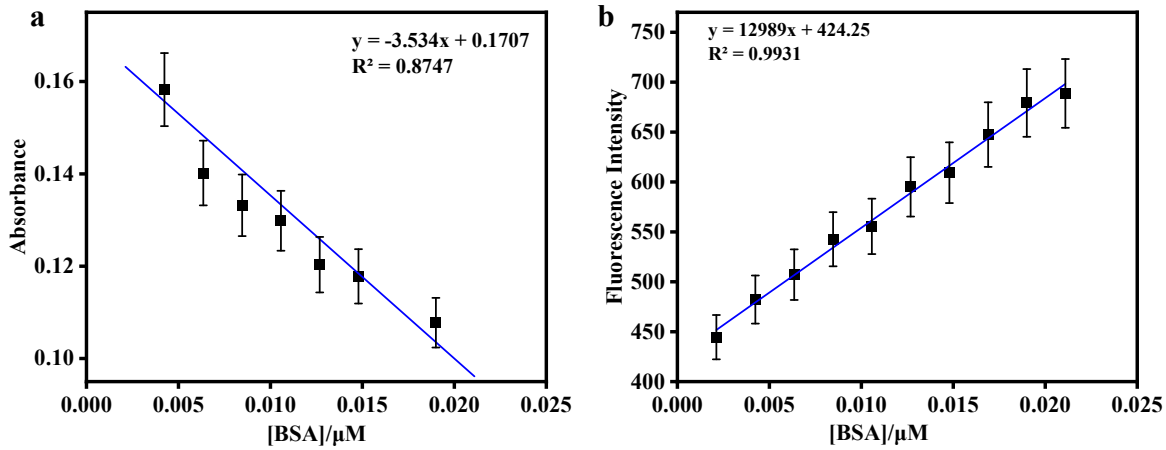


**Figure S6.** Changes of absorbance (a) and emission (b) **DSM** ($c$ = 2.0 × $10^{-5}$ M) upon addition of BSA ($c$ = 7.4μM).

From UV-*vis* (a) and fluorescence titration (b) of **DSM** with Ovalbumin (Fig.S7), slope values are -2.9701, 11101 and Sb1 values are 0.0054, 19.377 respectively.

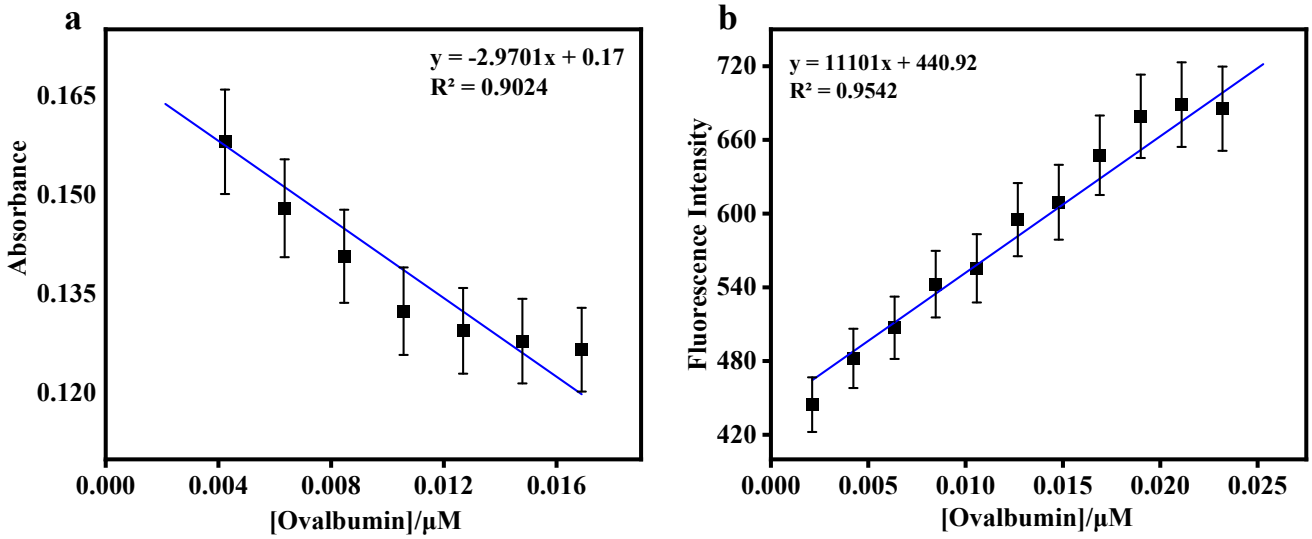


**Figure S7.** Changes of absorbance (a) and emission (b) of **DSM** ($c$ = 2.0 × $10^{-5}$ M) upon addition Ovalbumin ($c$ = 4.24 μM).

Thus, using the formula we have calculated the detection limit for **DSM** with DNA from UV-*vis* and fluorescence titration 2.79 μM, 1.01 μM respectively and **DSM** with BSA from UV-*vis*

and fluorescence titration 0.007 µM, 0.017 µM respectively and **DSM** with ovalbumin from UV-*vis* and fluorescence titration 0.005µM ,0.005µM respectively.

## 6.Jobs plot analysis:

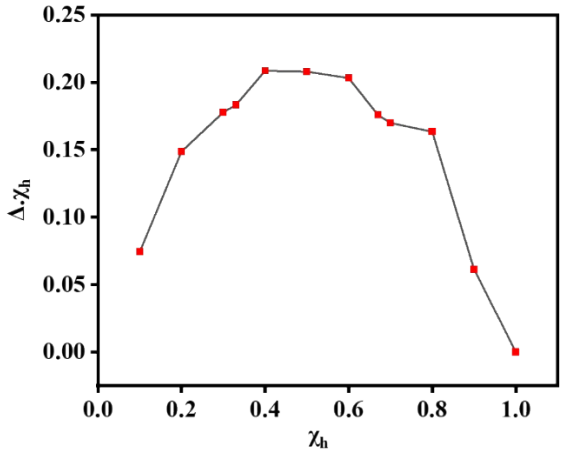


**Figure S8.** Job's plot diagram of receptor **DSM** for $Ni^{2+}$ (where Xh is the mole fraction of host **DSM** and ΔI indicates the change of the intensity).

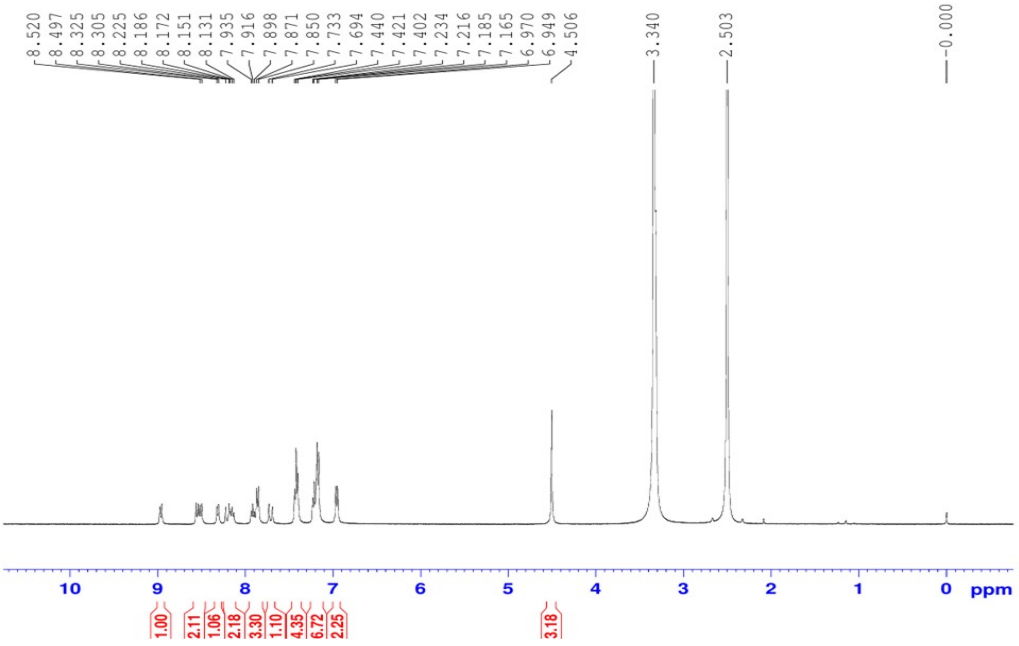


**Figure S9.** $^{1}H$ NMR spectrum of **DSM**

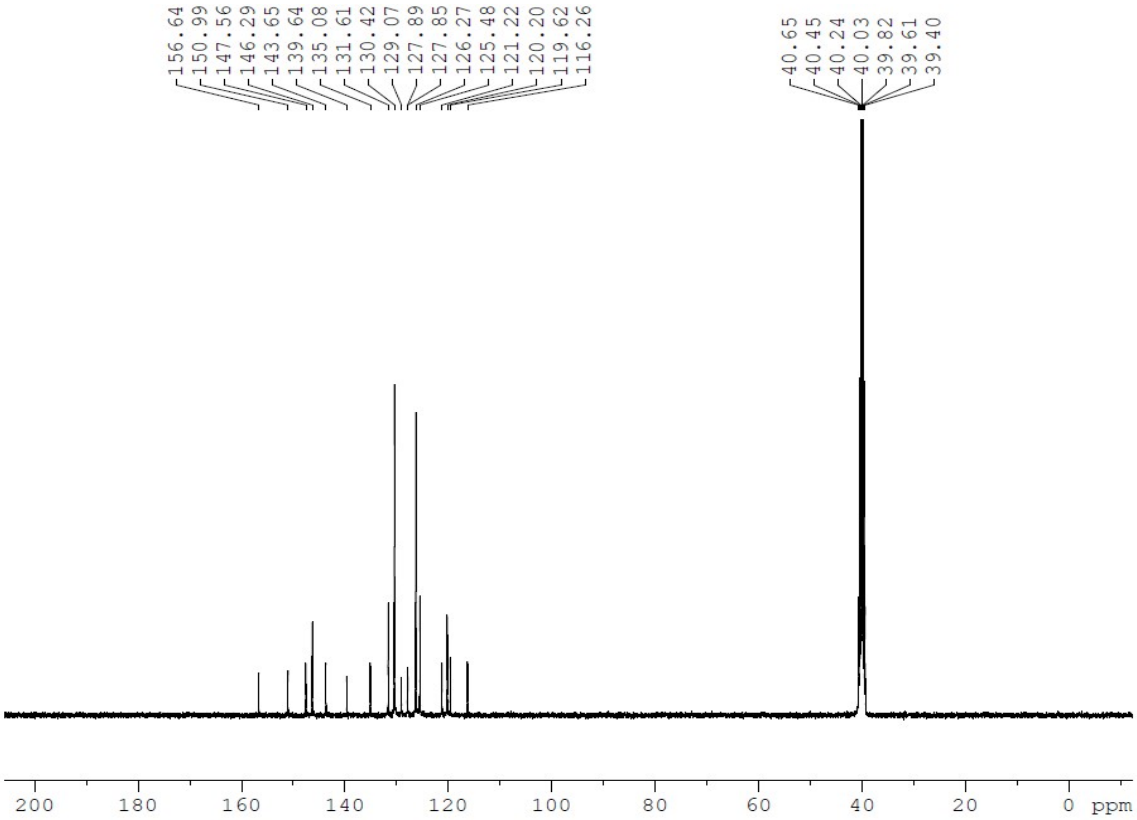


**Figure S10.** $^{13}$C-NMR spectrum of **DSM**

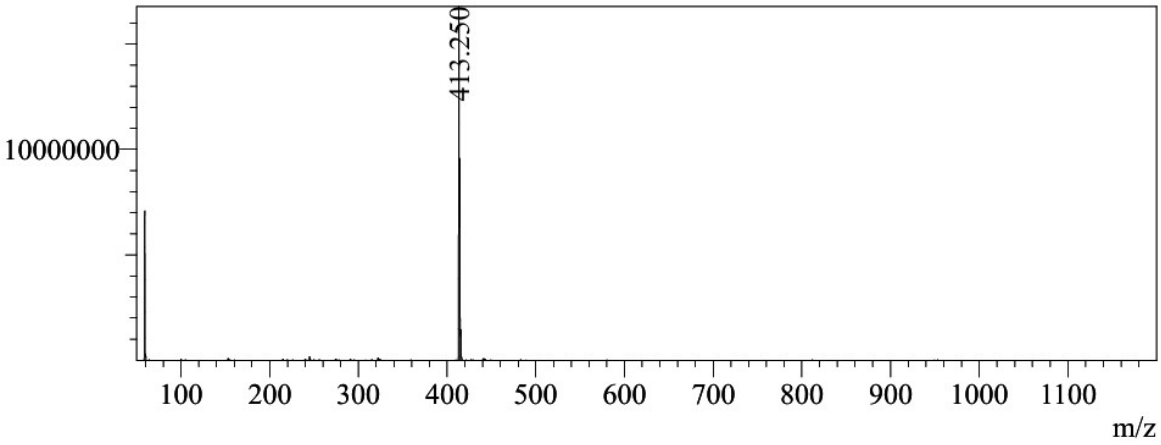


**Figure S11.** Mass spectrum of **DSM**

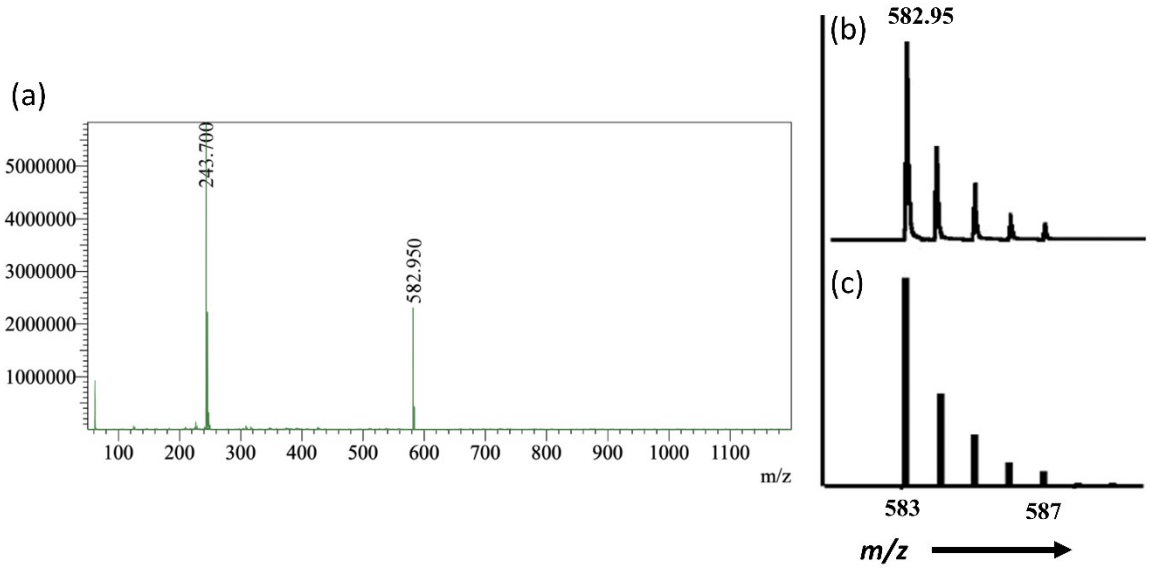


**Figure S12.** (a) Mass spectrum of **DSM**+$Ni^{2+}$ complex. (b) Signal at *m/z* 582.95 for **DSM**+$Ni^{2+}$ complex. c) Calculated isotopic distribution for **DSM**+$Ni^{2+}$ complex.

**Figure S13.** Photograph of TLC plates with **DSM** itself (left) and presence of $Ni^{2+}$ (right).

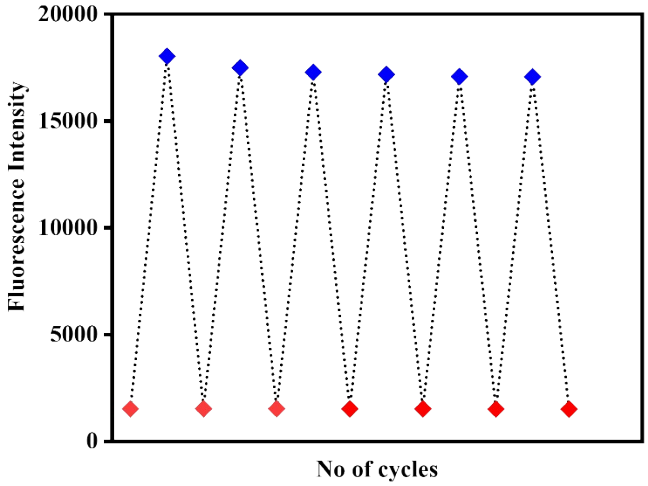


**Figure S14:** Reversibility cycle for DSM+$Ni^{2+}$ complex (blue squares) and DSM+$Ni^{2+}$ +$Na_2EDTA$ (red squares).

## 10. Computational details

### Methods for DFT

Density Functional Theory (DFT)[2] calculations were conducted using the Gaussian 09 (Revision A.02) package, with "Gauss View" utilized for visualizing molecular orbitals. Becke's three-parameter hybrid-exchange functional, the Lee-Yang-Parr expression for nonlocal correlation, and the Vosko-Wilk-Nuair 1980 local correlation functional (B3LYP) were employed in the calculation.[3] Optimization of **DSM** and single-point energy calculations in the gas phase were performed using the 6-31+(g) basis set. The Lanl2dz basis set was used for $Ni^{2+}$ and for H atoms we used 6-31+(g) basis set; for C, N, O, Cl, Ni atoms we employed LanL2DZ as basis set for all the calculations. The calculated electron-density plots for frontier molecular orbitals were prepared by using Gauss View 5.1 software. All the calculations were performed with the Gaussian 09W software package.[4]

### Methods for silico molecular docking studies

The three-dimensional structures of Bovine Serum Albumin (PDB id 4JK4, 2.65 Å, X-ray diffraction) protein and double helical DNA (PDB id 3K5N, 3.15 Å, X-ray diffraction) were downloaded from RCSB PDB (https://www.rcsb.org/). The structures are prepared for docking by using Swiss PDB viewer software. The molecular docking between the ligand and the target molecules (BSA and DNA) were performed by AutoDock Vina software as per our previously published work (Vishnu et al., 2024).[5] There three- and two-dimensional (interaction) rendering of BSA-ligand, and DNA-ligand complexes were performed by UCSF ChimeraX and Biovia Discovery Studio 2024, respectively.

## 11. Comparison table of DSM with the reported chemosensors (Table S1)

| Ligands | Analytes | Solvent Used | Probe type | Detection limit | Applications | Ref: |
|---|---|---|---|---|---|---|
| 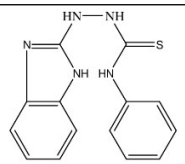 | $Ni^{2+}$ | $CH_3CN$-$H_2O$ | Turn on | $7.9\times10^{-8}$ M | $Ni^{2+}$ ion detection in different water samples | 6 |
| 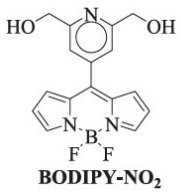 BODIPY-$NO_2$ | $Ni^{2+}$ | $CH_3CN$ | Turn-off | $1.7 \times 10^{-7}$M | - | 7 |
| 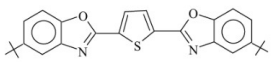 | $Ni^{2+}$ | Acetate buffer solution | Turn-off | $8.0 \times10^{-9}$M. | Determination of $Ni^{2+}$ in waste water samples | 8 |
| 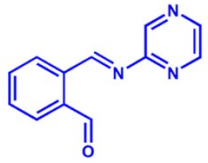 | $Ni^{2+}$ | MeOH/$H_2O$ | Turn-off | $8.62 \times 10^{-7}$M | Detection of $Ni^{2+}$ ion in aqueous solution | 9 |
| 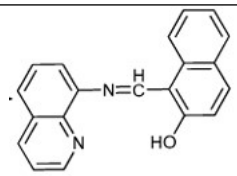 | $Ni^{2+}$ | DMSO–$H_2O$ | - | $5.0 \times10^{6}$ M | Dipstick method | 10 |
| 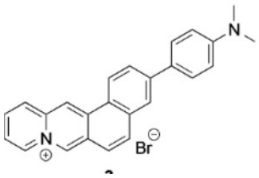 | ct-DNA BSA | BPE Buffer | Turn-on | - | Fluorometric Analysis of Cells | 11 |
| 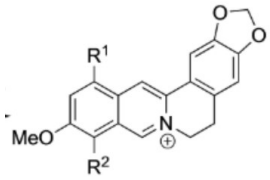 | ct-DNA | BPE buffer | Turn-on | - | fluorimetric detection of DNA in cells | 12 |

| | | | | | | |
|---|---|---|---|---|---|---|
| 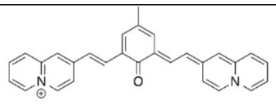 | ct-DNA | BPE-buffer | Turn-on | - | fluorimetric detection of DNA in cells | 13 |
| 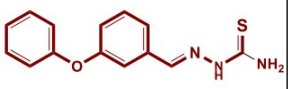 | ct-DNA, BSA | Tris HCl | Tur-On | - | - | 14 |
| 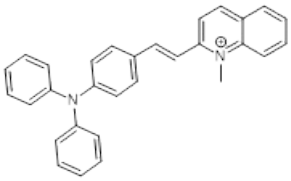 | $Ni^{2+}$, ct-DNA, BSA, and ovalbumin | $CH_3CN$-HEPES buffer ($Ni^{2+}$) Tris–HCl buffer (ct-DNA, BSA, and ovalbumin) | Turn on | 1.53 µM ($Ni^{2+}$) 1.01 µM (ct-DNA) 0.017 µM (BSA) 0.005µM (ovalbumin) | DFT and molecular docking | **This work** |

## 12. References:


1. F. H. Stootman, D. M. Fisher, A. Rodger, J. R. Aldrich-Wright, *Analyst*., 2006, **131**, 1145.
2 R. G. Parr and W. Yang, *Density Functional Theory of Atoms and Molecules*, Oxford University Press, Oxford, 1989.
3 (a) A. D. Becke, *J. Chem. Phys.,* 1993, **98**, 5648. (b) C. Lee , W. Yang and R. G. Parr, *Phys. Rev. B*, 1998, **37**, 785.
4 M. J. Frisch, G. W. Trucks, H. B. Schlegel, G. E. Scuseria, M. A. Robb, J. R. Cheeseman, G. Scalmani, V. Barone, B. Mennucci, G. A. Petersson, H. Nakatsuji, M. Caricato, X. Li, H. P. Hratchian, A. F. Izmaylov, J. Bloino, G. Zheng, J. L. Sonnenberg, M. Hada, M. Ehara, K. Toyota, R. Fukuda, J. Hasegawa, M. Ishida, T. Nakajima, Y. Honda, O. Kitao, H. Nakai, T. Vreven, J. A. Montgomery Jr., J. E. Peralta, F. Ogliaro, M. Bearpark, J. J. Heyd, E. Brothers, K. N. Kudin, V. N. Staroverov, R. Kobayashi, J. Normand, K. Raghavachari, A. Rendell, J. C. Burant, S. S. Iyengar, J. Tomasi, M. Cossi, N. Rega, J. M. Millam, M. Klene, J. E. Knox, J. B. Cross, V. Bakken, C. Adamo, J. Jaramillo, R. Gomperts, R. E. Stratmann, O. Yazyev, A. J. Austin, R. Cammi, C. Pomelli, J. W. Ochterski, R. L. Martin, K. Morokuma, V. G. Zakrzewski,

G. A. Voth, P. Salvador, J. J. Dannenberg, S. Dapprich, A. D. Daniels, Ö. Farkas, J. B. Foresman, J. V Ortiz, J. Cioslowski and D. J. Fox, Gaussian Inc., 2009, Wallingford CT.

5 S. Vishnu, A. Nag and A. K. Das, *Anal. Methods*, **2024**,16, 5263-5271.

6 M.R. Ganjali, M. Hosseini [c], M. Motalebi, M. Sedaghat, F. Mizani, F. Faridbod, P. No rouzi, *Spectrochimica Acta Part A: Molecular and Biomolecular Spectroscopy*, 2015, **140**, 283-287.

7 P. J. Huang, K. Kumarasamy, T. Devendhiran, Y. C. Chen, T. Y. Dong, M. C. Lin, *Journal of Molecular Structure*, 2021, **1246**, 131281.

8 M. Shamsipur, T. Poursaberi, A. R. Karami, M. Hosseini, A. Momeni, N. Alizadeh, M. Yousefi, M. R. Ganjali, *Analytica Chimica Acta*, 2004, **501**, 55-60

9 P. J. Huang, K. Kumarasamy, T. Devendhiran, Y. C. Chen, T. Y. Dong, M. C. Lin, *Journal of Molecular Structure*, 2021, **1246**, 131281.

10 M. Dhanushkodi, G. G. Vinoth K. Balakrishnan, K. Balachandar, S. Sarveswari, S. Gandhi, J. Rajesh , *Dyes and Pigments*, 2020, **173**, 107897

11 X. Liu, Q. Lin, T. -B. Wei and Y. M. Zhang, *New J. Chem.*, 2014, **38**, 1418-1423.

12 P. J. Wickhorst, Dr. S. I. Druzhinin, H. Ihmels, M. Müller, M. S. Sardo, H. Schönherr, G. Viola, *ChemPhotoChem* 2021, **5**, 1079 – 1088.

13 P. J. Wickhorst, H. Ihmels, *Chem. Eur. J.* 2021, **27**, 8580 – 8589.

14 A. K. Das, S. I. Druzhinin, H. Ihmels, M. Müller, H. Schönherr, *Chem. Eur. J.* 2019, **25**, 12703 – 12707.